

Deep Learning Based Sphere Decoding

Mostafa Mohammadkarimi, *Member, IEEE*, Mehrtash Mehrabi, *Student Member, IEEE*,
 Masoud Ardkani, *Senior Member, IEEE*, and Yindi Jing, *Member, IEEE*

Abstract—In this paper, a deep learning (DL)-based sphere decoding algorithm is proposed, where the radius of the decoding hypersphere is learnt by a deep neural network (DNN). The performance achieved by the proposed algorithm is very close to the optimal maximum likelihood decoding (MLD) over a wide range of signal-to-noise ratios (SNRs), while the computational complexity, compared to existing sphere decoding variants, is significantly reduced. This improvement is attributed to DNN’s ability of intelligently learning the radius of the hypersphere used in decoding. The expected complexity of the proposed DL-based algorithm is analytically derived and compared with existing ones. It is shown that the number of lattice points inside the decoding hypersphere drastically reduces in the DL-based algorithm in both the average and worst-case senses. The effectiveness of the proposed algorithm is shown through simulation for high-dimensional multiple-input multiple-output (MIMO) systems, using high-order modulations.

Index Terms—Sphere decoding, integer least-squares problem, maximum likelihood decoding, deep learning, deep neural network, multiple-input multiple-output, complexity analysis.

I. INTRODUCTION

THE problem of optimum maximum likelihood decoding (MLD) in spatial multiplexing multiple-input multiple-output (MIMO) systems leads to an integer least-squares (LS) problem, which is equivalent to finding the closest lattice point to a given point [1], [2]. The integer LS problem is much more challenging compared to the conventional LS problem, where the unknown vector is an arbitrary complex vector, and the solution is easily obtained through pseudo inverse. This is because of the discrete search space of the integer LS problem which makes it NP hard in both the worst-case sense and the average sense [3].

Various suboptimal solutions, such as zero-forcing (ZF) receiver, minimum mean squared error (MMSE) receiver, nulling and cancelling (NC), NC with optimal ordering, have been proposed for the integer LS problem in MIMO systems with reduced computational complexity [4]. These solutions first solve the unconstrained LS problem and then perform simple rounding to obtain a feasible lattice point. While these solutions result in cubic-order complexity, their performance is significantly worse than the optimal solution.

The idea of sphere decoding for MIMO detection was introduced in [5]. Sphere decoding suggests to confine the search space of the original integer LS problem to a hypersphere and

M. Mohammadkarimi, M. Mehrabi, M. Ardkani, and Y. Jing are with the Department of Electrical and Computer Engineering, University of Alberta, Edmonton, AB, Canada. (e-mail: {mostafa.mohammadkarimi, mehrtash, ardkani, yindi}@ualberta.ca).

This research was supported by the Huawei Innovation Research Program (HIRP).

implement a branch-and-bound search over a tree to achieve MLD performance. It can reduce the number of lattice points to be trialled, thus lower the complexity. Naturally, choosing an appropriate radius for the decoding hypersphere is crucial for sphere decoding. If the radius is too small, there might not be any lattice point inside the hypersphere. On the other hand, an overly large radius may result in too many lattice points in the hypersphere, hence increasing the decoding complexity. For example, the choice of radius based on the Babai estimate guarantees the existence of at least one lattice point inside the hypersphere [6]; however, it may lead to a large number of points within the hypersphere. To achieve the exact MLD performance with reduced complexity, sphere decoding with increasing radius search (SDIRS) was proposed in [3], [7].

Many variations of sphere decoding with reduced computational complexity have also been proposed in the literature [8]–[17]. Complexity reduction in sphere decoding through lattice reduction, geometric and probabilistic tree pruning, and K -based lattice selection methods have been addressed in [8]–[17]. On the other hand, a few studies have addressed the problem of radius selection in sphere decoding [3], [6]. A method to determine the radius of the decoding hypersphere was proposed in [3]. The proposed algorithm chooses the radii based on the noise statistics; however, it ignores the effect of the fading channel matrix. A modified version of radius selection based on Babai estimate has been developed in [6]. The proposed method can solve the problem of sphere decoding failure due to rounding error in floating-point computations. To take the advantage of sphere decoding for high-dimensional MIMO systems with high-order modulations and other applications, such as multi-user communications, massive MIMO, and relay communications [18]–[20], a promising solution is to develop an intelligent mechanism for radius selection to reduce computational complexity without performance degradation.

Recent studies show that deep learning (DL) can provide significant performance improvement in signal processing and communications problems [21]–[28]. Specifically, DL techniques have been employed to improve certain parts of conventional communication systems, such as decoding, modulation, and more [21]–[23]. These improvements are related to the intrinsic property of a deep neural network (DNN), which is a universal function approximator with superior logarithmic learning ability and convenient optimization capability [29]. Besides, existing signal processing algorithms in communications, while work well for systems with tractable mathematical models, can become inefficient for complicated and large-scale systems with large amount of imperfections and high nonlinearities. Such scenarios can be solved through DL,

which can characterize imperfections and nonlinearities via well-structured approximations [24]–[28].

Motivated by these facts, a sphere decoding algorithm based on DL is proposed in this paper, where the radius of the decoding hypersphere is learned by a DNN prior to decoding. The DNN maps a sequence of the fading channel matrix elements and the received signals at its input layer into a sequence of learned radiiuses at its output layer. The DNN is trained in an off-line procedure for the desired signal-to-noise ratio (SNR) once and is used for the entire communication phase.

Unlike the SDIRS algorithm, the proposed DL-based algorithm restricts the number of sequential sphere decoding implementations to a maximum predefined value. Moreover, since the decoding radiiuses are intelligently learnt by a DNN, the number of lattice points that lies inside the hypersphere remarkably decreases, which significantly reduces the computational complexity. On the other hand, the probability of failing to find a solution is close to zero. To the best of our knowledge, this is the first work in the literature that proposes a mechanism for radius selection dependent on both the fading channel matrix and the noise statistics.

The remaining of this paper is organized as follows. Section II briefly introduces the basics of DL and DNN. Section III presents the system model. Section IV describes the proposed DL-based sphere decoding algorithm. In Section V, an analytical expression for the expected complexity of the proposed algorithm is derived. Simulation results are provided in Section VI, and conclusions are drawn in Section VII.

A. Notations

Throughout the paper, $(\cdot)^*$ is used for the complex conjugate, $(\cdot)^T$ is used for transpose, $(\cdot)^H$ is used for Hermitian, $|\cdot|$ represents the absolute value operator¹ $\lfloor \cdot \rfloor$ is the operation that rounds a number to its closest integer, \emptyset denotes the empty set, $\mathbb{E}\{\cdot\}$ is the statistical expectation, \hat{x} is an estimate of x , the symbol \mathbf{I} denotes the identity matrix, and the Frobenius norm of vector \mathbf{a} is denoted by $\|\mathbf{a}\|$.

The inverse of matrix \mathbf{A} is denoted by \mathbf{A}^{-1} . $\text{Re}\{\cdot\}$ and $\text{Im}\{\cdot\}$ denote real and imaginary operands, respectively. The gradient operator is denoted by ∇ . The m -dimensional complex, real, and complex integer spaces are denoted by \mathbb{C}^m , \mathbb{R}^m , and \mathbb{CZ}^m , respectively. Finally, the circularly symmetric complex Gaussian distribution with mean vector $\boldsymbol{\mu}$ and covariance matrix $\boldsymbol{\Sigma}$ is denoted by $\mathcal{CN}(\boldsymbol{\mu}, \boldsymbol{\Sigma})$.

II. DNN FOR DEEP LEARNING

Deep learning is a subset of artificial intelligence and machine learning that uses multi-layered nonlinear processing units for feature extraction and transformation. On the contrary to the conventional machine learning techniques, the performance of the DL techniques significantly improve as the number of training data increases. Most of the modern DL techniques have been developed based on artificial neural network and are referred to as DNN.

¹For the sets, it represents the cardinality.

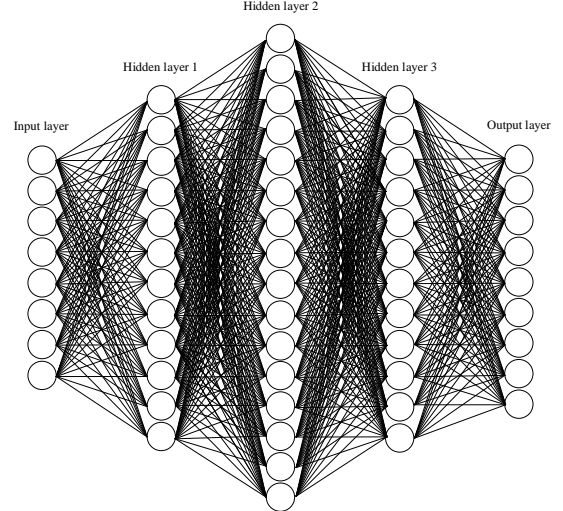


Fig. 1: A typical DNN with three hidden layers.

A DNN is a fully connected feedforward neural network (NN) composed of several hidden layers and the neurons between the input and output layers. It is distinguished from the conventional NN by its depth, i.e., the number of hidden layers and the number of neurons. A larger number of hidden layers and neurons enables a DNN to extract more meaningful features and patterns from the data. From a mathematical point of view, a DNN is a “universal approximator”, because it can learn to approximate any function $\mathbf{z} = \Upsilon(\mathbf{x})$ mapping the input $\mathbf{x} \in \mathbb{R}^m$ to the output $\mathbf{z} \in \mathbb{R}^n$. By employing a cascade of L nonlinear transformations on the input \mathbf{x} , a DNN approximates \mathbf{z} as

$$\mathbf{z} \approx T_{(L)}\left(T_{(L-1)}\left(\cdots T_1(\mathbf{x}; \boldsymbol{\theta}_1); \boldsymbol{\theta}_{L-1}\right); \boldsymbol{\theta}_L\right), \quad (1)$$

with

$$T_{(\ell)}(\mathbf{x}; \boldsymbol{\theta}_\ell) \triangleq A_\ell(\mathbf{W}_\ell \mathbf{x} + \mathbf{b}_\ell), \quad \ell = 1, \dots, L, \quad (2)$$

where $\boldsymbol{\theta}_\ell \triangleq (\mathbf{W}_\ell \mathbf{b}_\ell)$ denotes the set of parameters, $\mathbf{W}_\ell \in \mathbb{R}^{n_\ell \times n_{\ell-1}}$ (where $n_0 = m$, $n_L = n$) and $\mathbf{b}_\ell \in \mathbb{R}^{n_\ell}$ represents the weights and biases, and A_ℓ is the activation function of the ℓ th layer. The activation function is individually applied to each element of its input vector in order to produce nonlinearity. The weights and biases are usually learned through a training set with known desired outputs [29]. Fig. 1 shows a typical DNN with three hidden layers.

III. SYSTEM MODEL

We consider a spatial multiplexing MIMO system with m transmit and n receive antennas. The vector of received basedband symbols, $\mathbf{y} \in \mathbb{C}^{n \times 1}$, in block-fading channels is modeled as

$$\mathbf{y} = \mathbf{H}\mathbf{s} + \mathbf{w}, \quad (3)$$

where $\mathbf{s} = [s_1, s_2, \dots, s_m]^T \subset \mathbb{CZ}^m$ denotes the vector of transmitted complex symbols drawn from an arbitrary constellation \mathbb{D} , $\mathbf{H} \in \mathbb{C}^{n \times m}$ is the channel matrix, and

$\mathbf{w} \in \mathbb{C}^{n \times 1}$ is the zero-mean additive white Gaussian noise (AWGN) with covariance matrix $\Sigma_{\mathbf{w}} = \sigma_{\mathbf{w}}^2 \mathbf{I}$. The channel from transmit antenna j to receive antenna i is denoted by h_{ij} .

The vector \mathbf{s} spans the “rectangular” m -dimensional complex integer lattice $\mathbb{D}^m \subset \mathbb{CZ}^m$, and the n -dimensional vector \mathbf{Hs} spans a “skewed” lattice for any given lattice-generating matrix \mathbf{H} . With the assumption that \mathbf{H} is perfectly estimated at the receiver, MLD of the vector \mathbf{s} in (3) given the observation vector \mathbf{y} , leads to the following integer LS problem:

$$\min_{\mathbf{s} \in \mathbb{D}^m \subset \mathbb{CZ}^m} \|\mathbf{y} - \mathbf{Hs}\|^2. \quad (4)$$

As seen, the integer LS problem in (4) is equivalent to finding the closest point in the skewed lattice \mathbf{Hs} to the vector \mathbf{y} in the Euclidean sense. For large values of m and high-order modulation, exhaustive search is computationally unaffordable.

Sphere decoding can speed up the process of finding the optimal solution by searching only the points of the skewed lattice that lie within a hypersphere of radius d centered at the vector \mathbf{y} . This can be mathematically expressed as

$$\min_{\substack{\mathbf{s} \in \mathbb{D}^m \subset \mathbb{CZ}^m \\ \|\mathbf{y} - \mathbf{Hs}\|^2 \leq d^2}} \|\mathbf{y} - \mathbf{Hs}\|^2. \quad (5)$$

It is obvious that the closest lattice point inside the hypersphere is also the closest point for the whole lattice. The main problem in sphere decoding is how to choose d to avoid a large number of lattice points inside the hypersphere and at the same time guarantee the existence of a lattice point inside the hypersphere for any vector \mathbf{y} .

To achieve MLD error performance, SDIRS is required since for any hypersphere radius r_i , there is always a non-zero probability that this hypersphere does not contain any lattice point. When no lattice point is available, the search radius needs to be increased from r_i to r_{i+1} , and the search is conducted again. This procedure continues until the optimal solution is obtained. While SDIRS substantially improve on the complexity of MLD from an implementation standpoint, the average and worst-case complexity can still be huge when there are no lattice points in the hypersphere with radius r_i , but many in the hypersphere with radius r_{i+1} . Hence, the choice of r_i ’s is critical.

IV. DL-BASED SPHERE DECODING

The main idea behind our proposed DL-based sphere decoding algorithm is to implement SDIRS for a small number of intelligently learned radii. That is, r_i ’s are learned and chosen intelligently by a DNN. DL-based sphere decoding makes it possible to choose the decoding radii based on the noise statistics and the structure of \mathbf{H} . This significantly increases the probability of successful MLD with searching over only a small number of lattice points.

In the proposed DL-based sphere decoding, the Euclidean distance of the q closest lattice points to vector \mathbf{y} in the skewed lattice space is reconstructed via a DNN (as the DNN output) prior to sequential sphere decoding implementations. Then, these q learned Euclidean distances are used as radii of

the hyperspheres in sphere decoding implementations. The value of q is chosen small due to computational complexity consideration. Ideally, if the distances are produced with no error, $q = 1$ is sufficient for the optimal decoding with the lowest complexity, since the radius is the distance of \mathbf{y} to the optimal MLD solution. This radius for sphere decoding guarantees the existence of a point inside the hypersphere and actually only the optimal point is inside the hypersphere. However, since a DNN is an approximator, there is the possibility that no points lies within the hypersphere with the learned radius. Thus, instead of learning the closest distance only, q closest Euclidean distances are learnt by the DNN to increase the probability of finding the optimal lattice point. Since for any finite value of q , still there is the possibility that no lattice point lies within the hypersphere with the largest learned radius, a suboptimal detector, such as MMSE with rounding or NC with optimal ordering is employed in order to avoid failure in decoding.

Let us define the Euclidean distance between \mathbf{y} and the i th lattice point in the skewed lattice, i.e., \mathbf{Hs}_i , as

$$r_i \triangleq \|\mathbf{y} - \mathbf{Hs}_i\|, \quad i = 1, 2, \dots, |\mathbb{D}|^m, \quad (6)$$

where $|\mathbb{D}|$ is the cardinality of the constellation \mathbb{D} . Further, by ordering r_i as follows,

$$r_{i_1} < r_{i_2} < \dots < r_{i_q} < r_{i_{q+1}} < \dots < r_{i_{|\mathbb{D}|^m}}, \quad (7)$$

the desired $q \times 1$ radius vector \mathbf{r} is given as

$$\mathbf{r} \triangleq [r_{i_1} \ r_{i_2} \ \dots \ r_{i_q}]^T. \quad (8)$$

In the proposed DL-based sphere decoding algorithm, the DNN, $\Phi(\mathbf{x}; \boldsymbol{\theta})$, reconstructs the radius vector \mathbf{r} at its output layer as

$$\hat{\mathbf{r}} = \Phi(\mathbf{x}; \boldsymbol{\theta}), \quad (9)$$

where

$$\mathbf{x} \triangleq [\bar{\mathbf{y}} \ \bar{\mathbf{y}} \ \bar{h}_{11} \ \tilde{h}_{11} \dots \ \bar{h}_{nm} \ \tilde{h}_{nm}]^T, \quad (10)$$

$\bar{\mathbf{y}} = \text{Re}\{\mathbf{y}^T\}$, $\tilde{\mathbf{y}} = \text{Im}\{\mathbf{y}^T\}$, $h_{uv} \triangleq \bar{h}_{uv} + i\tilde{h}_{uv}$, and $\boldsymbol{\theta} \triangleq [\theta_1, \theta_2, \dots, \theta_K]^T$. The vector \mathbf{x} represents the input vector of the DNN, and $\boldsymbol{\theta}$ is the vector of all parameters of the DNN.

The proposed DL-based sphere decoding is composed of an off-line training phase, where the parameters of the DNN is obtained by employing training examples, and a decoding phase where the transmit vector is decoded through sphere decoding or a suboptimal detector. In the following subsection, these two phases are explained in details.

A. Training Phase

A three layers DNN with one hidden layer is considered for the training phase, where the numbers of neurons in each layers are $2n(m+1)$, 128, and q , respectively. Clipped rectified linear unit with the following mathematical operation is used as the activation function in the hidden layers:

$$f(u) = \begin{cases} 0, & u < 0. \\ u, & 0 \leq u < 1. \\ 1, & u \geq 1 \end{cases} \quad (11)$$

Algorithm 1 DL-based sphere decoding algorithm

Input: $\mathbf{y}, \mathbf{H}, \Phi(\cdot, \boldsymbol{\theta}), q$
Output: $\hat{\mathbf{s}}$

- 1: Stack \mathbf{y} and \mathbf{H} as in (10) to obtain \mathbf{x} ;
- 2: Obtain the q radiuses through the trained DNN as $\hat{\mathbf{r}} = \Phi(\mathbf{x}, \boldsymbol{\theta}) = [\hat{r}_{i_1} \hat{r}_{i_2} \cdots \hat{r}_{i_q}]^T$;
- 3: $c = 1$;
- 4: Implement sphere decoding for radius \hat{r}_{i_c} ;
- 5: **if** $D_{\text{sp}}(\mathbf{y}, \hat{r}_{i_c}) \neq \text{null}$
- 6: $\hat{\mathbf{s}} = D_{\text{sp}}(\mathbf{y}, \hat{r}_{i_c})$;
- 7: **else**
 - 8: **if** $c < q$
 - 9: $c = c + 1$ and go to 4;
 - 10: **else**
 - 11: $\hat{\mathbf{s}} = D_{\text{sb}}(\mathbf{y})$;
 - 12: **end**
 - 12: **end**

It should be mentioned that an SNR dependent DNN, in which the structure of the DNN is designed to be adaptive to the SNR value, can also be employed to further reduce computational complexity. For the sake of simplicity, the structure of the DNN is considered the same for all SNR values in this paper.

In the training phase, the designed DNN is trained with independent input vectors, given as

$$\mathbf{x}^{(i)} \triangleq \left[\bar{\mathbf{y}}^{(i)} \bar{\mathbf{y}}^{(i)} \bar{h}_{11}^{(i)} \tilde{h}_{11}^{(i)} \cdots \bar{h}_{nm}^{(i)} \tilde{h}_{nm}^{(i)} \right]^T \quad (12)$$

for $i = 1, 2, \dots, N$ to obtain the parameter vector $\boldsymbol{\theta}$ of the DNN by minimizing the following mean-squared error (MSE) loss function:

$$\text{Loss}(\boldsymbol{\theta}) \triangleq \frac{1}{N} \sum_{i=1}^N \left\| \mathbf{r}^{(i)} - \Phi(\mathbf{x}^{(i)}; \boldsymbol{\theta}) \right\|^2, \quad (13)$$

where $\mathbf{r}^{(i)}$ is the desired radius vector when $\mathbf{x}^{(i)}$ is used as input vector. To achieve faster convergence and decrease computational complexity, an approximation of the MSE loss function in (13) is computed for mini-batches of training examples at each iteration t as

$$f_t(\boldsymbol{\theta}) \triangleq \frac{1}{M} \sum_{i=1}^M \left\| \mathbf{r}^{(M(t-1)+i)} - \Phi(\mathbf{x}^{(M(t-1)+i)}; \boldsymbol{\theta}) \right\|^2, \quad (14)$$

where M is the mini-batch size, and $B = N/M$ is the number of batches. By choosing M to be considerably small compared to N , the complexity of the gradient computation for one epoch, i.e., $\nabla_{\boldsymbol{\theta}} f_t(\boldsymbol{\theta}_{t-1})$, $t = 1, 2, \dots, B$, remarkably decreases when compared to $\nabla_{\boldsymbol{\theta}} \text{Loss}(\boldsymbol{\theta})$, while the variance of the parameter update still decreases.

During the training phase, for each SNR value, elements of the transmitted vector $\mathbf{s}^{(i)}$, elements of the fading channel matrix $\mathbf{H}^{(i)}$, and elements of the noise vector $\mathbf{w}^{(i)}$, $i = 1, \dots, N$, are independently and uniformly drawn from \mathbb{D} , $f_h(h)$, and $\mathcal{CN}(0, \sigma_w^2)$, respectively, where $f_h(h)$ denotes the distribution of the fading channel. Then, the real and imaginary parts of the observation vectors during training, i.e., $\mathbf{y}^{(i)} = \mathbf{H}^{(i)} \mathbf{s}^{(i)} + \mathbf{w}^{(i)}$, along with $\mathbf{H}^{(i)}$ are stacked as in (12)

and fed to the DNN to minimize the MSE loss function in (14). For each input training vector $\mathbf{x}^{(i)}$, the corresponding desired radius vector $\mathbf{r}^{(i)}$ is obtained by employing SDIRS with a set of heuristic radiuses. Finally, the parameter vector of the DNN is updated according to the input-output vector pairs $(\mathbf{x}^{(i)}, \mathbf{r}^{(i)})$ by employing the adaptive moment estimation stochastic optimization algorithm, which is also referred to as Adam algorithm [30].

The details of the Adam algorithm can be described as follows. At the t th iteration, $t = 1, \dots, B$, the i th parameter θ_i is updated as

$$\theta_{i,t} = \theta_{i,t-1} - \eta \frac{\hat{\alpha}_{i,t}}{\sqrt{\hat{\delta}_{i,t} + \epsilon}}, \quad (15)$$

where $\boldsymbol{\theta}_0 = [\theta_{1,0}, \theta_{2,0}, \dots, \theta_{K,0}]^T$ is random initial value, η is the learning rate that determines the step size of the update and

$$\hat{\alpha}_{i,t} \triangleq \frac{\alpha_{i,t}}{1 - \beta_1^t} \quad (16a)$$

$$\hat{\delta}_{i,t} \triangleq \frac{\delta_{i,t}}{1 - \beta_2^t} \quad (16b)$$

$$\alpha_{i,t} \triangleq \beta_1 \alpha_{i,t-1} + (1 - \beta_1) g_{i,t} \quad (16c)$$

$$\delta_{i,t} \triangleq \beta_2 \delta_{i,t-1} + (1 - \beta_2) g_{i,t}^2 \quad (16d)$$

$$g_{i,t} \triangleq \nabla_{\boldsymbol{\theta}_i} f_t(\boldsymbol{\theta}_{t-1}) \quad (16e)$$

with β_1 , β_2 , and ϵ being constant values. Appropriate default settings are $\beta_1 = 0.9$, $\beta_2 = 0.999$, and $\epsilon = 10^{-8}$. Empirical results demonstrate that Adam algorithm works well compared to other stochastic optimization methods, such as RMSProp [31]. In particular, it exhibits a fast convergence and does not stuck at saddle points by considering the past gradients during the parameters update.

B. Decoding Procedure

In the decoding phase, first, the received vector \mathbf{y} and fading channel matrix \mathbf{H} are fed to the trained DNN in the form of (10) to produce the radius vector $\hat{\mathbf{r}} \triangleq [\hat{r}_{i_1} \hat{r}_{i_2} \cdots \hat{r}_{i_q}]^T$; then, the transmitted signal vector is decoded by Algorithm 1, where sphere decoding is conducted recursively with the learned radiuses by the DNN, followed by a suboptimal detection if the sphere decoding fails to find the solution. Sphere decoding implementation with decoding radius \hat{r}_{i_c} fails to find a solution when

$$\mathcal{C}(\mathbf{y}, \hat{r}_{i_c}) \triangleq \left\{ \mathbf{s} \in \mathbb{D}^m \mid \left\| \mathbf{y} - \mathbf{H}\mathbf{s} \right\|^2 \leq \hat{r}_{i_c}^2 \right\} = \emptyset \quad (17)$$

that is, there is no lattice point inside the hypersphere with radius \hat{r}_{i_c} . To help the presentation, define

$$D_{\text{sp}}(\mathbf{y}, \hat{r}_{i_c}) \triangleq \begin{cases} \min_{\mathbf{s} \in \mathbb{D}^m \subset \mathbb{C}\mathbb{Z}^m} \left\| \mathbf{y} - \mathbf{H}\mathbf{s} \right\|^2, & \text{if } \mathcal{C}(\mathbf{y}, \hat{r}_{i_c}) \neq \emptyset \\ \text{null}, & \text{if } \mathcal{C}(\mathbf{y}, \hat{r}_{i_c}) = \emptyset. \end{cases} \quad (18)$$

$$\begin{aligned}
C_{\text{DL}}(m, \sigma^2) &= \lim_{U \rightarrow \infty} \frac{1}{U} \sum_{u=1}^U \sum_{c=1}^q \sum_{k=1}^m \sum_{v=0}^{\infty} F_{\text{sp}}(k) \Psi_{2k}(v) \times \gamma\left(\frac{\hat{r}_{i_c, u}^2}{\sigma_w^2 + v}, n - m + k\right) \left(\gamma\left(\frac{\hat{r}_{i_c, u}^2}{\sigma_w^2}, n\right) - \gamma\left(\frac{\hat{r}_{i_{c-1}, u}^2}{\sigma_w^2}, n\right)\right) \\
&\quad + \left(m^3 + \frac{5m^2}{2} + nm^2 + 3mn - \frac{m}{2}\right) \left(1 - \frac{1}{U} \sum_{u=1}^U \gamma\left(\frac{\hat{r}_{i_q, u}^2}{\sigma_w^2}, n\right)\right) + F_{\text{dn}}.
\end{aligned} \tag{24}$$

On the other hand, if no point is found by the q rounds of sphere decoding, MMSE is employed as the suboptimal detector, in which the solution is obtained as

$$D_{\text{sb}}(\mathbf{y}) = \left[(\mathbf{H}^H \mathbf{H} + \bar{\gamma}^{-1} \mathbf{I})^{-1} \mathbf{H}^H \mathbf{y} \right], \tag{19}$$

where $\bar{\gamma}$ is the average SNR. Simulation result show that due to the intelligent production of the radiiuses via a DNN, the probability of decoding through suboptimal detector is very close to zero.

V. EXPECTED COMPLEXITY OF THE DL-BASED SPHERE DECODING

In this section, the expected complexity of the proposed DL-based sphere decoding algorithm in the decoding phase is analytically derived. Since the DNN is trained once and is used for the entire decoding phase, the expected complexity of the training phase is not considered.

Lemma 1. *The expected complexity of the proposed DL-based sphere decoding algorithm is obtained as*

$$\begin{aligned}
C_{\text{DL}}(m, \sigma^2) &= \sum_{c=1}^q \sum_{k=1}^m \sum_{v=0}^{\infty} F_{\text{sp}}(k) \Psi_{2k}(v) \\
&\times \mathbb{E} \left\{ \gamma\left(\frac{\hat{r}_{i_c}^2}{\sigma_w^2 + v}, n - m + k\right) \left(\gamma\left(\frac{\hat{r}_{i_c}^2}{\sigma_w^2}, n\right) - \gamma\left(\frac{\hat{r}_{i_{c-1}}^2}{\sigma_w^2}, n\right)\right) \right\} \\
&+ \left(1 - \mathbb{E} \left\{ \gamma\left(\frac{\hat{r}_{i_q}^2}{\sigma_w^2}, n\right) \right\}\right) F_{\text{sb}} + F_{\text{dn}},
\end{aligned} \tag{20}$$

where $\hat{r}_{i_0} = 0$, $\gamma(\cdot, \cdot)$ is the lower incomplete gamma function, $\Psi_{2k}(v)$ is the number of ways that v can be represented as the sum of $2k$ squared integers,

$$F_{\text{sb}} = m^3 + \frac{5m^2}{2} + nm^2 + 3mn - \frac{m}{2}, \tag{21}$$

$$F_{\text{dn}} = \sum_{i=0}^{L-1} 2n_{i+1}n_i, \tag{22}$$

and $F_{\text{sp}}(k)$ is the number of elementary operations including complex additions, subtractions, and multiplications per visited point in complex dimension k in sphere decoding.

Proof. See the appendix. \square

As seen from the proof in the appendix, F_{sb} and F_{dn} represents the number of elementary operations employed by the MMSE suboptimal detector in (19) and DNN, respectively. Also, the term $\gamma(\hat{r}_{i_c}^2/\sigma_w^2, n)$ in (20) is the probability of finding

at least a lattice point inside the hypersphere with the learned radius \hat{r}_{i_c} , which is written as

$$\hat{p}_{i_c} \triangleq \gamma\left(\frac{\hat{r}_{i_c}^2}{\sigma_w^2}, n\right) = \int_0^{\frac{\hat{r}_{i_c}^2}{\sigma_w^2}} \frac{t^{n-1}}{\Gamma(n)} \exp(-t) dt, \tag{23}$$

where $\hat{p}_{i_0} = 0$.

By replacing the statistical expectation with sample mean based on importance sampling, one can write the expected complexity of the DL-based algorithm as in (24), where the subscript u represents the index of sample in importance sampling.

For M^2 -QAM constellation, $F_{\text{sp}}(k) = 8k + 20 + 4M$, and $\Psi_{2k}(v)$ for 4-QAM, 16-QAM, and 64-QAM is respectively given as [32]

$$\Psi_{2k}(v) = \begin{cases} \binom{2k}{v}, & \text{if } 0 \leq v \leq 2k \\ 0, & \text{otherwise,} \end{cases} \tag{25}$$

$$\Psi_{2k}(v) = \begin{cases} \sum_{j=0}^{2k} \frac{1}{2^{2k}} \binom{2k}{j} \Omega_{2k,j}(v), & \text{if } v \in \Xi \\ 0, & \text{otherwise,} \end{cases} \tag{26}$$

and

$$\Psi_{2k}(v) = \begin{cases} \sum_{\xi_0, \xi_1, \xi_2, \xi_3} \frac{1}{4^{2k}} \Omega_{2k, \xi_0, \xi_1, \xi_2, \xi_3}(v), & \text{if } v \in \mathcal{Q} \\ 0, & \text{otherwise} \end{cases} \tag{27}$$

where $\Omega_{2k,j}(v)$ is the coefficient of λ^v in the polynomial

$$(1 + \lambda + \lambda^4 + \lambda^9)^j (1 + 2\lambda + \lambda^4)^{2k-j}, \tag{28}$$

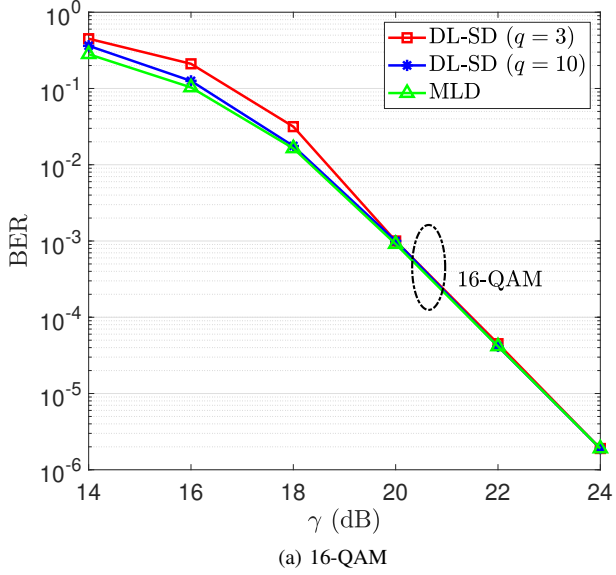
the set Ξ contains the coefficients of the polynomial in (28) for $k = 1, \dots, m$ and $j = 0, \dots, 2k$, $\Omega_{2k, \xi_0, \xi_1, \xi_2, \xi_3}(v)$ is the coefficient of λ^v in the polynomial

$$\begin{aligned}
&\binom{2k}{\xi_0, \xi_1, \xi_2, \xi_3} \left(\sum_{e_0=0}^7 \lambda^{e_0^2} \right)^{\xi_0} \left(\lambda + \sum_{e_1=0}^6 \lambda^{e_1^2} \right)^{\xi_1} \\
&\times \left(\lambda + \lambda^4 + \sum_{e_2=0}^5 \lambda^{e_2^2} \right)^{\xi_2} \left(-1 - \lambda^{16} + \sum_{e_3=0}^4 2\lambda^{e_3^2} \right)^{\xi_3},
\end{aligned} \tag{29}$$

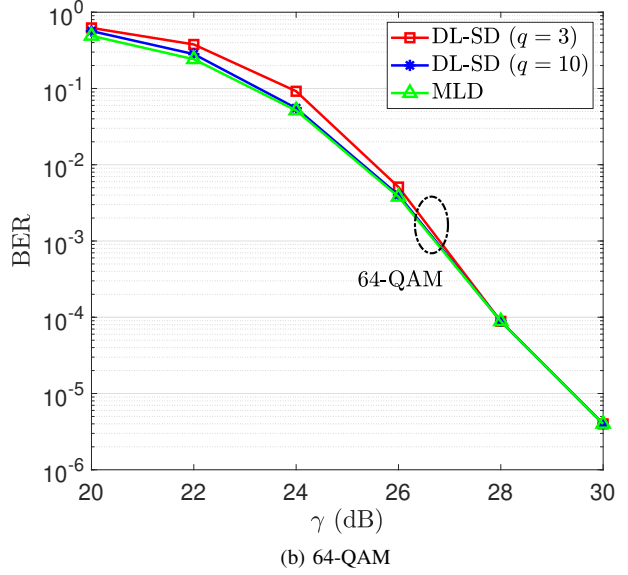
where $\xi_0 + \xi_1 + \xi_2 + \xi_3 = 2k$, $\binom{2k}{\xi_0, \xi_1, \xi_2, \xi_3} = (2k)!/(\xi_0! \xi_1! \xi_2! \xi_3!)$, and the set \mathcal{Q} contains the coefficients of the polynomial in (29) for $k = 1, \dots, m$.

VI. SIMULATION RESULTS

In this section, we evaluate the performance of the proposed DL-based sphere decoding algorithm through several simulation experiments.



(a) 16-QAM



(b) 64-QAM

Fig. 2: Performance comparison of the proposed DL-based sphere decoding algorithm ($q = 3$ and $q = 10$) and the SDIRS (MLD performance) in [32].

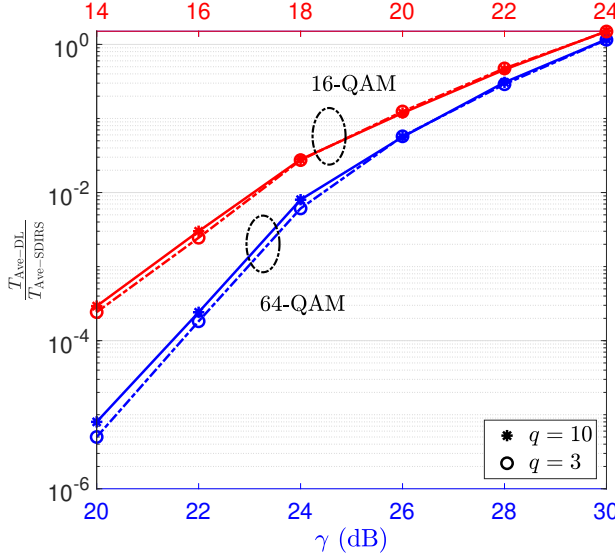


Fig. 3: Ratio of the average decoding time in the proposed DL-based algorithm, $T_{\text{Ave-DL}}$, to the average decoding time in the SDIRS algorithm, $T_{\text{Ave-SDIRS}}$, in [32].

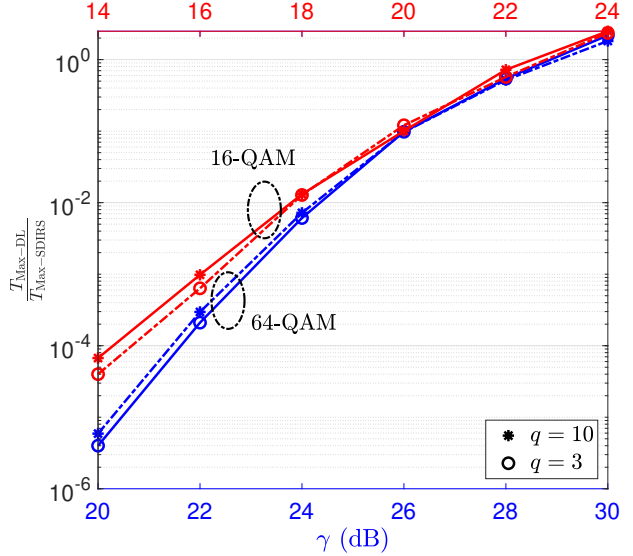


Fig. 4: Ratio of the maximum decoding time in the proposed DL-based algorithm, $T_{\text{Max-DL}}$, to the maximum decoding time in the SDIRS, $T_{\text{Max-SDIRS}}$, in [32].

A. Simulation Setup

We consider a 10×10 spatial multiplexing MIMO system in Rayleigh block-fading channel where 16-QAM and 64-QAM are employed. These configurations result in skewed lattices with 4^{20} and 4^{40} lattice points, respectively. The elements of the fading channel matrix are modeled as independent and identically distributed (i.i.d.) zero-mean complex Gaussian random variables with unit variance. The additive white noise is modeled as a complex-valued Gaussian random variable with zero-mean and variance σ_w^2 for each receive antennas. Without loss of generality, the average SNR in dB is defined

as $\gamma \triangleq 10 \log \left(m\sigma_s^2 / \sigma_w^2 \right)$, where σ_s^2 is the average signal power. In the training phase, 1000 batches of training data, i.e., $B = 1000$, are employed where each batch contains $M = 20$ input vectors. The learning rate, η , of the Adam optimization algorithm is set as 0.001.

Unless otherwise mentioned, $q = 10$ and $q = 3$ are considered, and MMSE is employed as the suboptimal detector. The performance of the proposed DL-based sphere decoding algorithm in terms of bit error rate (BER) and computational complexity is obtained from 10^6 Monte Carlo trials for each SNR value. The computational complexity of the proposed

algorithm is evaluated in terms of average decoding time, maximum decoding time, and complexity exponent, which is defined as

$$e_c \triangleq \log \frac{C(m, \sigma_w^2)}{\log m}.$$

The performance comparison of the DL-based sphere decoding algorithm with the SDIRS algorithm in [32] is performed with the same sets of fading channel matrixes, transmit vectors, and noise vectors.

B. Simulation Results

Fig. 2 illustrates the BER of the proposed DL-based sphere decoding algorithm versus the average SNR. The MLD performance is also shown for comparison, which was obtained by employing SDIRS algorithm with $p_c(i) = 1 - 0.99^i$ at the i th sphere decoding implementation as suggested in [32]. As seen, the proposed DL-based algorithm exhibits BER performance close to that in MLD over a wide range of SNRs. This behaviour shows that sequential sphere decoding implementation with the learned radii reaches the optimal solution. Moreover, as seen, by increasing q , the BER decreases. However, the performance gap between the DL-based sphere decoding algorithm with $q = 3$ and the one with $q = 10$ is insignificant for higher SNR values. In other words, having $q = 3$ is sufficient to find a close-to-optimal result for BERs below 10^{-3} .

In Fig. 3, the ratio of the average decoding time in the proposed DL-based algorithm to the average decoding time in the SDIRS algorithm in [32] is shown. As seen, the average decoding time in the DL-based algorithm is significantly lower than the one in [32] when $14 \leq \gamma \leq 23.3$ dB for 16-QAM, and when $20 \leq \gamma \leq 29.8$ dB for 64-QAM. For example, this ratio is almost 10000 at 22 dB SNR for 64-QAM. The reason for this reduction in complexity is that the number of lattice points inside the decoding hypersphere, and thus the size of the search tree decreases in the average sense when the radii of the hyperspheres are intelligently learnt by a DNN. On the other hand, the sphere decoding algorithm in [32] exhibits a lower computational complexity compared to the proposed DL-based algorithm when $\gamma > 23.3$ dB for 16-QAM, and when $\gamma > 29.8$ dB for 64-QAM. The reason is that at high SNR values, it is unlikely for the lattice to collapse in one or more dimension, an event that significantly increases the number of points in the hypersphere for the scheme in [32]. One possible way to improve the proposed method is to consider SNR-based DNN, especially at high SNR values.

Fig. 4 shows the ratio of the maximum decoding time in the proposed DL-based algorithm to that in the SDIRS algorithm in [32]. As seen, the DL-based sphere decoding algorithm outperforms the algorithm in [32]. This shows that the size of the search tree in the DL-based sphere decoding is much smaller than the one in the algorithm in [32] in the worst-case sense.

In Fig. 5, the average number of lattice points (in the logarithmic scale) falling inside the decoding hypersphere in

the DL-based sphere decoding algorithm is compared with the one in the SDIRS algorithm in [32]. As seen, the average number of lattice points in the DL-based algorithms is below 0.1761 (in the non logarithmic scale, below 1.5), while this is much higher in the SDIRS algorithm.

Fig. 6 compares the complexity exponent of the proposed DL-based sphere decoding algorithm in (24) with that of the algorithm in [32]. As expected, the DL-based algorithm exhibits a lower complexity exponent when the average SNR is below 23 dB. Also, its complexity exponent shows the same trend as its average decoding time in Fig. 3. This confirms the validity of the theoretical result in (24).

VII. CONCLUSION

A low-complexity solution for integer LS problems based on the capabilities of DL and sphere decoding algorithm was proposed in this paper. The proposed solution leads to efficient implementation of sphere decoding for a small set of intelligently learned radii. The BER performance of the DL-based sphere decoding algorithm is very close to that in MLD for high-dimensional integer LS problems with significantly lower computational complexity. The expected complexity of the proposed algorithm based on the elementary operations was derived, and its effectiveness in term of BER and computational complexity for high-dimensional MIMO communication systems, using higher-order modulations, was shown through simulation. While the integer LS problem in this paper was formulated for MIMO communication systems, it is a promising solution for other situations when integer LS problems are encountered, such as multi-user communications, relay communications and more.

APPENDIX I

The expected complexity of sphere decoding implementation for radius d is given as [32]

$$C(m, \sigma_w^2, d) = \sum_{k=1}^m F_{\text{sp}}(k) \sum_{v=0}^{\infty} \gamma\left(\frac{d^2}{\sigma_w^2 + v}, n - m + k\right) \Psi_{2k}(v). \quad (30)$$

By employing (30) and following the same procedure as in [32], the expected complexity of the SDIRS algorithm for $r_1 < r_2 < \dots < r_q$ is obtained as

$$C(m, \sigma_w^2, r_1, \dots, r_q) = \sum_{c=1}^q (p_c - p_{c-1}) \sum_{k=1}^m F_{\text{sp}}(k) \times \sum_{v=0}^{\infty} \gamma\left(\frac{r_c^2}{\sigma_w^2 + v}, n - m + k\right) \Psi_{2k}(v), \quad (31)$$

where $p_0 = 0$, and p_c , $0 < c \leq q$, is the probability of finding at least a lattice point inside the hypersphere with radius r_c , which is obtained by replacing r_c with \hat{r}_{i_c} in (23).

The probability that a solution is not found during the sphere decoding implementation for the hyperspheres with radii r_1, r_2, \dots, r_q equals $(1 - p_q)$. Hence, the proposed DL-based sphere decoding algorithm obtains the solution through a suboptimal detector with probability $(1 - p_q)$. This leads to $(1 - p_q)F_{\text{sb}}$ additional average complexity given a

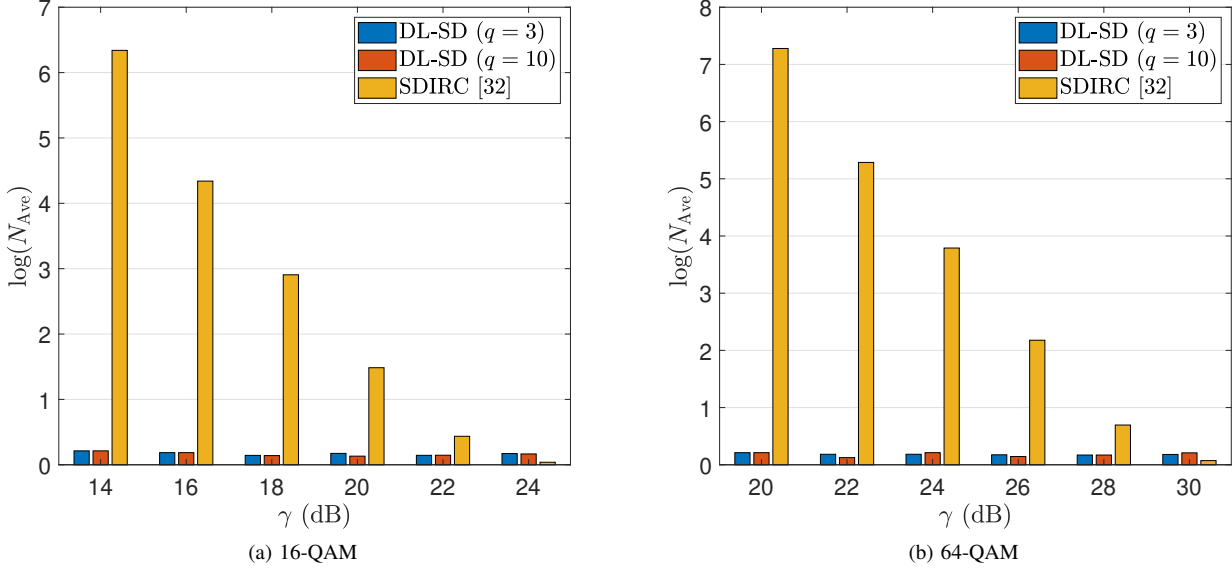


Fig. 5: The average number of lattice points (in the logarithmic scale) falling inside the search hypersphere in the DL-based sphere decoding algorithm and the SDIRC algorithm in [32].

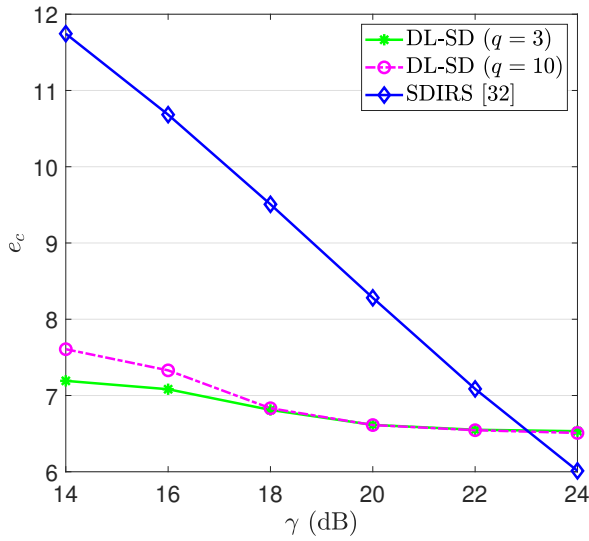


Fig. 6: Complexity component of the proposed DL-based algorithm ($q = 3$ and $q = 10$) and the SDIRS algorithm in [32] for 16-QAM modulation.

suboptimal detector with F_{sb} elementary operations. For the MMSE detector in (19), the number of elementary operations of $(\mathbf{H}^H \mathbf{H} + \bar{\gamma}^{-1} \mathbf{I})$ is $nm^2 + m(n - \frac{m}{2}) + \frac{m}{2}$, the matrix inversion in (19) requires $m^3 + m^2 + m$ elementary operations, $\mathbf{H}^H \mathbf{y}$ requires $m(2n - 1)$ elementary operations, and the product of $(\mathbf{H}^H \mathbf{H} + \bar{\gamma}^{-1} \mathbf{I})^{-1}$ and $\mathbf{H}^H \mathbf{y}$ requires $2m^2 - m$ elementary operations [33]. Thus, the total elementary operations in the MMSE detection is given as in (21).

Moreover, there is F_{dn} elementary operations due to the DNN computations. The number of multiplication and addition

in the ℓ th layer of a DNN with n_ℓ neurons is $2n_\ell n_{\ell-1}$, where $n_{\ell-1}$ is the number of neurons in the $(\ell - 1)$ th layer. Hence, for a L -layer DNN with n_0, \dots, n_L neurons in each layer, F_{dn} is given as in (22).

By employing (31) and including $(1 - p_q)F_{\text{sb}}$ and F_{dn} , the expected complexity of the proposed DL-based sphere decoding algorithm given the learned radii $\hat{r}_{i_1}, \dots, \hat{r}_{i_q}$ is obtained as

$$C_{\text{DL}}(m, \sigma_w^2, \hat{r}_{i_1}, \dots, \hat{r}_{i_q}) = \sum_{c=1}^q (\hat{p}_{i_c} - \hat{p}_{i_{c-1}}) \sum_{k=1}^m F_{\text{sp}}(k) \times \sum_{v=0}^{\infty} \gamma \left(\frac{\hat{r}_{i_c}^2}{\sigma_w^2 + v}, n - m + k \right) \Psi_{2k}(v) + (1 - \hat{p}_{i_q}) F_{\text{sb}} + F_{\text{dn}}, \quad (32)$$

where \hat{p}_{i_c} is given in (23). Finally, since $\hat{r}_{i_1}, \dots, \hat{r}_{i_q}$ and thus $\hat{p}_{i_1}, \dots, \hat{p}_{i_q}$ are random variables, one can write the expected complexity of the DL-based sphere decoding as in (20).

REFERENCES

- [1] J. Jalden and P. Elia, "Sphere decoding complexity exponent for decoding full-rate codes over the quasi-static MIMO channel," *IEEE Trans. Inf. Theory*, vol. 58, no. 9, pp. 5785–5803, Sep. 2012.
- [2] J. Mietzner, R. Schober, L. Lampe, W. H. Gerstacker, and P. A. Hoeher, "Multiple-antenna techniques for wireless communications—a comprehensive literature survey," *IEEE Commun. Surveys Tuts.*, vol. 11, no. 2, Sencond quarter 2009.
- [3] B. Hassibi and H. Vikalo, "On the sphere-decoding algorithm I. expected complexity," *IEEE Trans. Signal Process.*, vol. 53, no. 8, pp. 2806–2818, Aug. 2005.
- [4] B. Hassibi, "An efficient square-root algorithm for BLAST," in *Proc. ICASSP*, vol. 2. IEEE, Aug. 2000, pp. 737–740.
- [5] E. Viterbo and J. Boutros, "A universal lattice code decoder for fading channels," *IEEE Trans. Inf. Theory*, vol. 45, no. 5, pp. 1639–1642, Jul. 1999.
- [6] F. Zhao and S. Qiao, "Radius selection algorithms for sphere decoding," in *Proc. CSSE*, Montreal, Canada, May 2009, pp. 169–174.

- [7] B. M. Hochwald and S. Ten Brink, "Achieving near-capacity on a multiple-antenna channel," *IEEE Trans. Commun.*, vol. 51, no. 3, pp. 389–399, 2003.
- [8] E. Agrell, T. Eriksson, A. Vardy, and K. Zeger, "Closest point search in lattices," *IEEE Trans. Inf. Theory*, vol. 48, no. 8, pp. 2201–2214, Aug. 2002.
- [9] A. M. Chan and I. Lee, "A new reduced-complexity sphere decoder for multiple antenna systems," in *Proc. ICC*, New York, USA, Apr. 2002, pp. 460–464.
- [10] L. G. Barbero and J. S. Thompson, "Fixing the complexity of the sphere decoder for MIMO detection," *IEEE Trans. Wireless Commun.*, vol. 7, no. 6, Jun. 2008.
- [11] B. Shim and I. Kang, "Sphere decoding with a probabilistic tree pruning," *IEEE Trans. Signal Process.*, vol. 56, no. 10, pp. 4867–4878, Oct. 2008.
- [12] R. Gowaikar and B. Hassibi, "Statistical pruning for near-maximum likelihood decoding," *IEEE Trans. Signal Process.*, vol. 55, no. 6, pp. 2661–2675, May 2007.
- [13] B. Shim and I. Kang, "Radius-adaptive sphere decoding via probabilistic tree pruning," in *proc. SPAWC*, Helsinki, Finland, Jun. 2007, pp. 1–5.
- [14] X.-W. Chang, J. Wen, and X. Xie, "Effects of the LLL reduction on the success probability of the babai point and on the complexity of sphere decoding," *IEEE Trans. Inf. Theory*, vol. 59, no. 8, pp. 4915–4926, Jun. 2013.
- [15] W. Zhao and G. B. Giannakis, "Sphere decoding algorithms with improved radius search," *IEEE Trans. Commun.*, vol. 53, no. 7, pp. 1104–1109, Jul. 2005.
- [16] H. Vikalo, B. Hassibi, and T. Kailath, "Iterative decoding for MIMO channels via modified sphere decoding," *IEEE Trans. Wireless Commun.*, vol. 3, no. 6, pp. 2299–2311, Nov. 2004.
- [17] Z. Yang, C. Liu, and J. He, "A new approach for fast generalized sphere decoding in MIMO systems," *IEEE Signal Process. Lett.*, vol. 12, no. 1, pp. 41–44, Jan. 2005.
- [18] Q. Wang and Y. Jing, "Performance analysis and scaling law of MR-C/MRT relaying with CSI error in multi-pair massive MIMO systems," *IEEE Trans. Wireless Commun.*, vol. 16, no. 9, pp. 5882–5896, Sep. 2017.
- [19] K. Mahdaviani, M. Ardash, and C. Tellambura, "On raptor code design for inactivation decoding," *IEEE Trans. Commun.*, vol. 60, no. 9, pp. 2377–2381, Sep. 2012.
- [20] S. Sun and Y. Jing, "Training and decodings for cooperative network with multiple relays and receive antennas," *IEEE Trans. Commun.*, vol. 60, no. 6, pp. 1534–1544, Jun. 2012.
- [21] H. Ye, G. Y. Li, and B.-H. Juang, "Power of deep learning for channel estimation and signal detection in OFDM systems," *IEEE Wireless Communications Letters*, vol. 7, no. 1, pp. 114–117, Feb. 2018.
- [22] E. Nachmani, E. Marciano, L. Lugosch, W. J. Gross, D. Burshtein, and Y. Be'ery, "Deep learning methods for improved decoding of linear codes," *IEEE J. Sel. Areas Commun.*, vol. 12, no. 1, pp. 119–131, Feb. 2018.
- [23] N. Farsad and A. Goldsmith, "Detection algorithms for communication systems using deep learning," *arXiv preprint arXiv:1705.08044*, 2017.
- [24] M. Kim, N.-I. Kim, W. Lee, and D.-H. Cho, "Deep learning aided SCMA," *IEEE Commun. Lett.*, vol. 22, no. 7, pp. 720–723, Apr. 2018.
- [25] T. O'Shea and J. Hoydis, "An introduction to deep learning for the physical layer," *IEEE Trans. on Cogn. Commun. Netw.*, vol. 3, no. 4, pp. 563–575, Dec. 2017.
- [26] S. Dörner, S. Cammerer, J. Hoydis, and S. ten Brink, "Deep learning based communication over the air," *IEEE J. Sel. Topics Signal Process.*, vol. 12, no. 1, pp. 132–143, Feb. 2018.
- [27] T. J. O'Shea, T. Erpek, and T. C. Clancy, "Deep learning based MIMO communications," *arXiv preprint arXiv:1707.07980*, 2017.
- [28] T. Wang, C.-K. Wen, H. Wang, F. Gao, T. Jiang, and S. Jin, "Deep learning for wireless physical layer: Opportunities and challenges," *China Communications*, vol. 14, no. 11, pp. 92–111, 2017.
- [29] I. Goodfellow, Y. Bengio, A. Courville, and Y. Bengio, *Deep learning*. MIT press Cambridge, 2016, vol. 1.
- [30] D. P. Kingma and J. Ba, "Adam: A method for stochastic optimization," *arXiv preprint arXiv:1412.6980*, 2014.
- [31] G. N. Vanderplaats, *Numerical optimization techniques for engineering design*. Vanderplaats Research and Development, Incorporated, 2001.
- [32] H. Vikalo and B. Hassibi, "On the sphere-decoding algorithm II. generalizations, second-order statistics, and applications to communications," *IEEE Trans. Signal Process.*, vol. 53, no. 8, pp. 2819–2834, Aug. 2005.
- [33] G. H. Golub and C. F. Van Loan, *Matrix computations*. JHU Press, 2012, vol. 3.